

# Effect of adding an imidized acrylic polymer to super tough nylon 6 on stiffness and toughness

T. Harada<sup>1</sup>, E. Carone Jr<sup>2</sup>, R.A. Kudva, H. Keskkula, D.R. Paul\*

*Department of Chemical Engineering and Texas Materials Institute, University of Texas at Austin, Austin, TX 78712, USA*

Received 15 June 1998; accepted 1 September 1998

## Abstract

The mechanical properties and phase morphology of ternary blends of nylon 6 with rubber, e.g., maleated ethylene-propylene random copolymer (EPR-g-MA) or maleated styrene-(ethylene-co-butylene)-styrene (SEBS-g-MA), and a rigid but brittle imidized acrylic polymer (IA) are explored. The objective was to investigate blends which have independently dispersed rubber and rigid polymer particles in a nylon 6 matrix. The amount of rubber was fixed at 20%, while the IA to nylon 6 ratio was varied. Addition of imidized acrylic polymer particles to nylon 6 toughened by EPR-g-MA particles leads to increased stiffness and room-temperature impact strength and does not change the ductile-to-brittle transition temperatures up to a critical level. Similar improvements in stiffness and room temperature impact strength were found for nylon 6 toughened by SEBS-type rubber; however, the low temperature impact properties were not as good. © 1999 Elsevier Science Ltd. All rights reserved.

*Keywords:* Nylon; EPR; SEBS

## 1. Introduction

There is extensive technical literature on rubber-toughened polyamides [1–16]. A variety of rubber types can be used for toughening polyamides; however, maleated ethylene-propylene random copolymers (EPR-g-MA) are among the most effective [12–14]. Reaction of the maleic anhydride with the polyamide amine end groups during melt processing [16] leads to graft copolymer formation which permits rather precise control of rubber particle size and improvement of the rubber-matrix interfacial strength. Super-tough blends that have low ductile–brittle transition temperatures can thus be achieved. A disadvantage of rubber toughening is the significant reduction of modulus or stiffness that accompanies the addition of the soft rubber phase to the rigid polyamide. Materials with a better balance between stiffness and impact strength are needed.

Inoue and others [17–21] have described blends of rigid polymer particles in a ductile polymer matrix which offer a route to increasing the modulus. Interestingly, the addition

of these rigid particles sometimes slightly improves rather than decreases impact strength. This stems from the fact that the small rigid particles are able to undergo shear yielding within the ductile matrix even though these rigid materials appear to be quite brittle when in the form of macroscopic samples. Blends of polyamides or other engineering thermoplastics with ABS materials or core-shell impact modifier are examples where both rubber and rigid materials, i.e. the styrene/acrylonitrile copolymer, SAN, phase of ABS or the poly(methyl methacrylate) shell of the emulsion-made impact modifiers are incorporated into a ductile matrix [22–31]. In these blends, the rubber particles are surrounded by rigid polymer and there are no matrix–rubber interfaces.

Another option is to have both rubber and rigid polymer particles distributed individually in the ductile matrix [32]. The question of interest is whether it is possible to generate super-tough compositions of improved stiffness by means of these two different kinds of dispersed phases in the matrix. The purpose of this paper is to investigate the mechanical properties and the morphology of such blends.

In this work, the matrix phase is nylon 6, the rigid particles are formed from an imidized acrylic polymer [23], and the rubber particles are formed from a maleated elastomer. Both the rigid and rubbery particles are quite small and are chemically bonded to the matrix by reaction of their anhydride units with the amine end groups of the polyamide.

\* Corresponding author. Tel.: +1-(512)-471-5392; fax: +1-(512)-471-0542.

<sup>1</sup> Permanent address: Mitsubishi Gas Chemical Co. Inc., 6-1-1 Niijuku Katsushika-ku Tokyo 171, Japan.

<sup>2</sup> Permanent address: State University of Campinas, CP: 6154 CEP: 13081-970 Campinas, SP, Brazil.

Table 1  
Materials used

Designation used here	Material (commercial designation)	Composition	Molecular weight	Relative melt viscosity <sup>a</sup>	Source
Nylon 6	Capron 8207F	End-group content; [NH <sub>2</sub> ] = 477.9 μeqS g <sup>-1</sup> ; [COOH] = 43.0 μeq g <sup>-1</sup>	$\bar{M}_n = 22,000$	1.0	AlliedSignal Inc.
EPR-g-MA	Exxelor 1803 53% Propylene 1.14 wt% MA	43% Ethylene	N/A	1.5	Exxon Chemical Co.
SEBS	Kraton G 1652	29% Styrene	Styrene block = 7,000 EB block = 37,500	1.6	Shell Chemical Co.
SEBS-g-MA	Kraton FG 1901X	29% Styrene 1.84 wt% MA	N/A	1.0	Shell Chemical Co.
Imidized acrylic polymer (IA)	EXL4140	55.7 wt% Methyl glutarimide 41.0 wt% Methyl methacrylate 2.18 wt% Methacrylic acid 1.08 wt% Glutaric anhydride	$\bar{M}_w = 95,000$	1.6	Rohm and Haas Co.

<sup>a</sup> Brabender torque at 245°C and 60 rev min<sup>-1</sup> after 10 min relative to nylon 6.

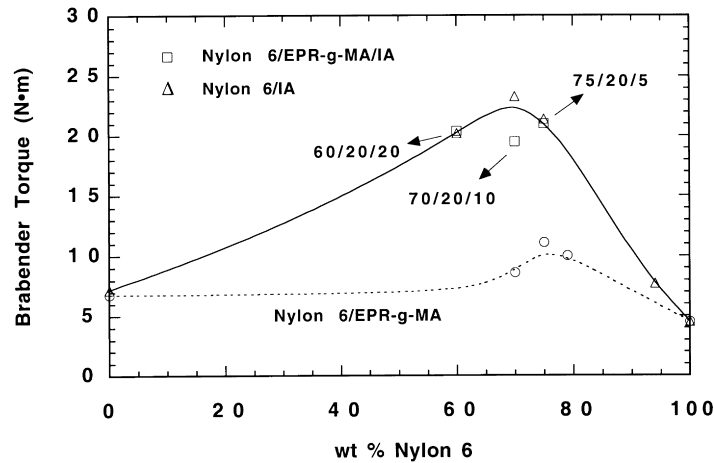


Fig. 1. Brabender torque of nylon 6/IA ( $\Delta$ ), nylon 6/EPR-g-MA ( $\circ$ ) and nylon 6/EPR-g-MA/IA ( $\square$ ) blends. Torque readings were taken after 10 min at 245°C and 60 rev min<sup>-1</sup>.

## 2. Experimental

Table 1 summarizes information about the various materials used in this work. The nylon 6 is a commercially available material with  $\bar{M}_n = 22,000$  and 47.9  $\mu\text{eq g}^{-1}$  of amine and 43.0  $\mu\text{eq g}^{-1}$  of carboxyl end-groups. Before each processing step, all materials containing nylon 6 were dried for at least 12 h at 85°C in a vacuum oven to ensure removal of sorbed water. The maleated ethylene-propylene rubber (EPR-g-MA) used contained 1.14 wt% grafted maleic anhydride while the maleated styrene-(ethylene-co-butylene)-styrene block copolymer (SEBS-g-MA) contained 1.84 wt% grafted maleic anhydride. The imidized acrylic polymer, made by reactive extrusion of PMMA with methyl amine, contained 1.08 wt% glutaric anhydride units and has been described more fully elsewhere [23].

For rheological characterization, the various polymers were tested in a Brabender Plasticorder outfitted with a 50 ml mixing head and standard rotors and operated at 245°C and 60 rev min<sup>-1</sup>. Binary and ternary blends were

prepared by simultaneous extrusion of all components (except where mentioned otherwise) in a Killion single-screw extruder (L/D = 30, 2.54 cm diameter) at 245°C using a screw speed of 40 rev min<sup>-1</sup>. To ensure adequate mixing, all blends were extruded twice. The extruded pellets were injection molded into standard 0.318 cm thick tensile (ASTM D638 type I) and Izod (ASTM D256) bars using an Arburg single screw injection molding machine. Mechanical properties were determined for samples in the dry as-molded state. Tensile testing was performed using an Instron in accordance with ASTM D638. An extensometer strain gauge with a 2 in (5.08 cm) gap was used to obtain the modulus and yield strain values at a crosshead speed of 0.2 in min<sup>-1</sup> (0.5 cm min<sup>-1</sup>). Elongation at break was determined from the crosshead travel rate assuming a gauge length of 9.65 cm and a crosshead speed of 2.0 in min<sup>-1</sup> (5.08 cm min<sup>-1</sup>). Notched Izod impact measurements were made using a TMI pendulum-type impact tester equipped with an insulated chamber for heating and cooling the specimens. At least three each of gate and far ends of the Izod bars were tested, i.e. 6 specimens. In many cases, the

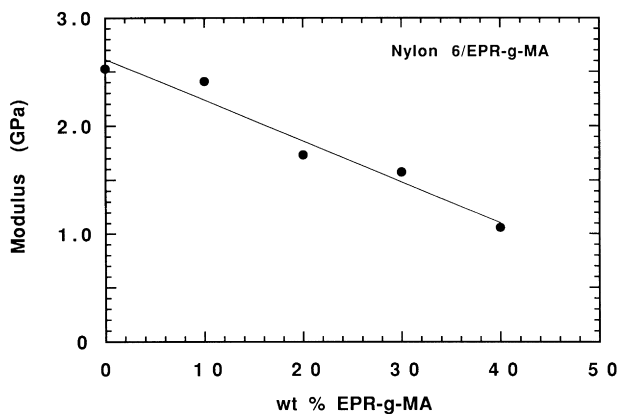


Fig. 2. Tensile modulus of nylon 6/EPR-g-MA blends as a function of EPR-g-MA content.

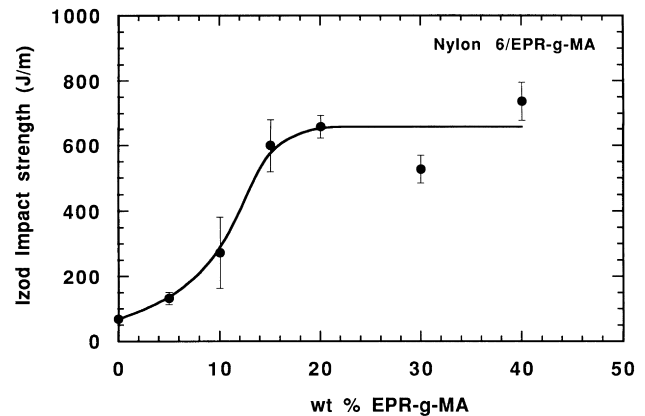


Fig. 3. Room-temperature Izod impact strength of nylon 6/EPR-g-MA blends as a function of EPR-g-MA content.

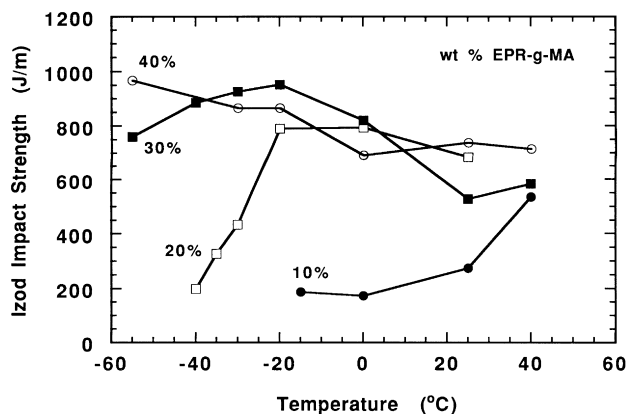


Fig. 4. Effect of temperature on the Izod impact strength of binary nylon 6/EPR-g-MA blends.

room-temperature impact strength of the gate end was higher than that of the far end (in the order of 10–20%). However, the qualitative trends in room-temperature impact strength shown here are independent of the end of the bar that is tested. The ductile-to-brittle transition temperatures of these blends were found to be independent of the end of the bar that was tested.

Blend morphologies were determined using a JEOL 200CX transmission electron microscope operating at an accelerating voltage of 120 kV. Samples were microtomed under cryogenic conditions ( $-45^{\circ}\text{C}$ ) into ultrathin sections (15–20 nm thick) from Izod bars perpendicular to the flow direction. Phase contrast between the blend components was achieved using various staining techniques. For binary nylon 6/IA blends, the sections were exposed to a 2% aqueous solution of phosphotungstic acid (PTA) to stain the polyamide phase. For the blends containing EPR-g-MA, the middle parts of Izod bars were trimmed with a mill and razor blade to form a block of approximately 5 mm  $\times$  5 mm  $\times$  2 mm. These blocks were further trimmed to the shape of a pyramid with the tip faced off to an area of 0.2 mm  $\times$  0.2 mm. These blocks were exposed to vapors of

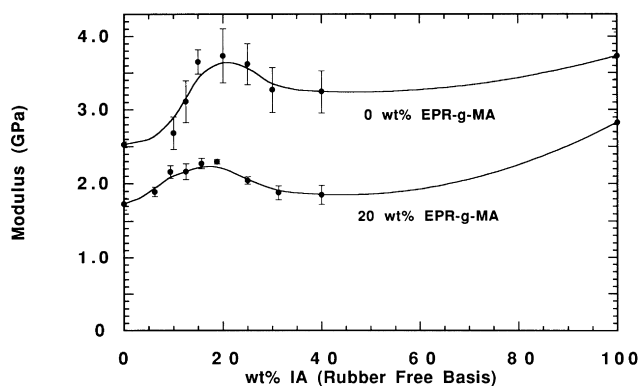


Fig. 5. Tensile modulus of binary nylon 6/IA blends (0% EPR-g-MA) and ternary nylon 6/EPR-g-MA/IA (20% EPR-g-MA) blends as a function of IA content on a rubber-free basis.

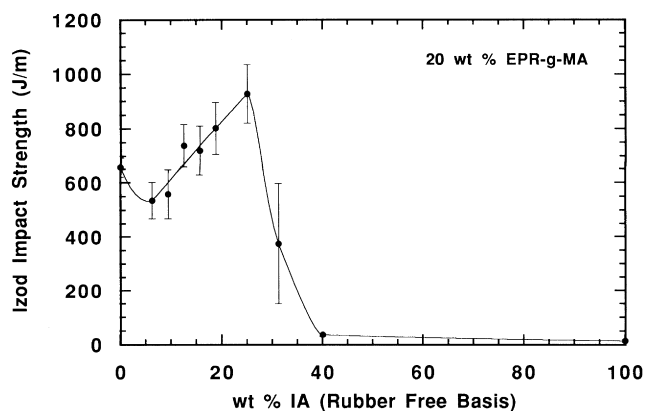


Fig. 6. Room-temperature Izod impact strength of ternary blends of nylon 6/EPR-g-MA/IA containing 20% EPR-g-MA as a function of IA content on a rubber-free basis.

*n*-pentyl benzene for a period of 5 h, following a procedure that is similar to one used by Gonzales-Montiel [33]. After that, the samples were stained before microtoming by exposure to vapors of an aqueous 0.5%  $\text{RuO}_4$  solution for a period of 12 h. The samples were then removed, cleaned with deionized water and dried in air. This procedure permitted preferential staining of the imidized acrylic polymer instead of the EPR-g-MA phase. After sectioning, PTA was used to stain the polyamide phase. For the materials containing SEBS-g-MA, blends were microtomed and the samples were exposed to either vapors of ruthenium tetroxide ( $\text{RuO}_4$ ) to stain the SEBS rubber or PTA to stain the polyamide phase. Photomicrographs of selected blends were employed for particle size analysis by a semi-automatic digital analysis technique based on Image® software from the National Institutes of Health. Weight average particle diameters,  $\bar{d}_w$ , were computed from these results. The average aspect ratio of the particles were calculated from the ratio of the major axis to minor axis of each particle. The crystallinity of nylon 6 in blends was determined by a Perkin-Elmer DSC-7 equipped with a thermal analysis

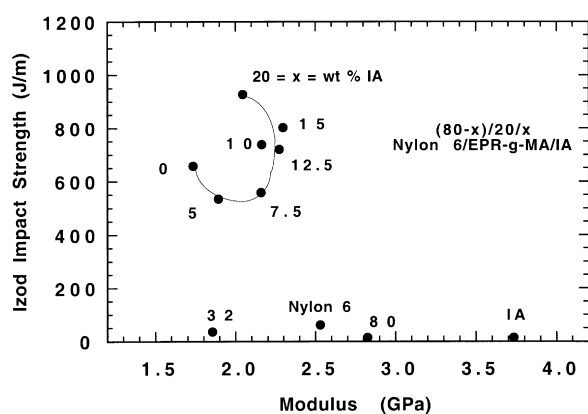


Fig. 7. Room-temperature Izod impact strength versus modulus of ternary blends of nylon 6/EPR-g-MA/IA containing 20% EPR-g-MA.

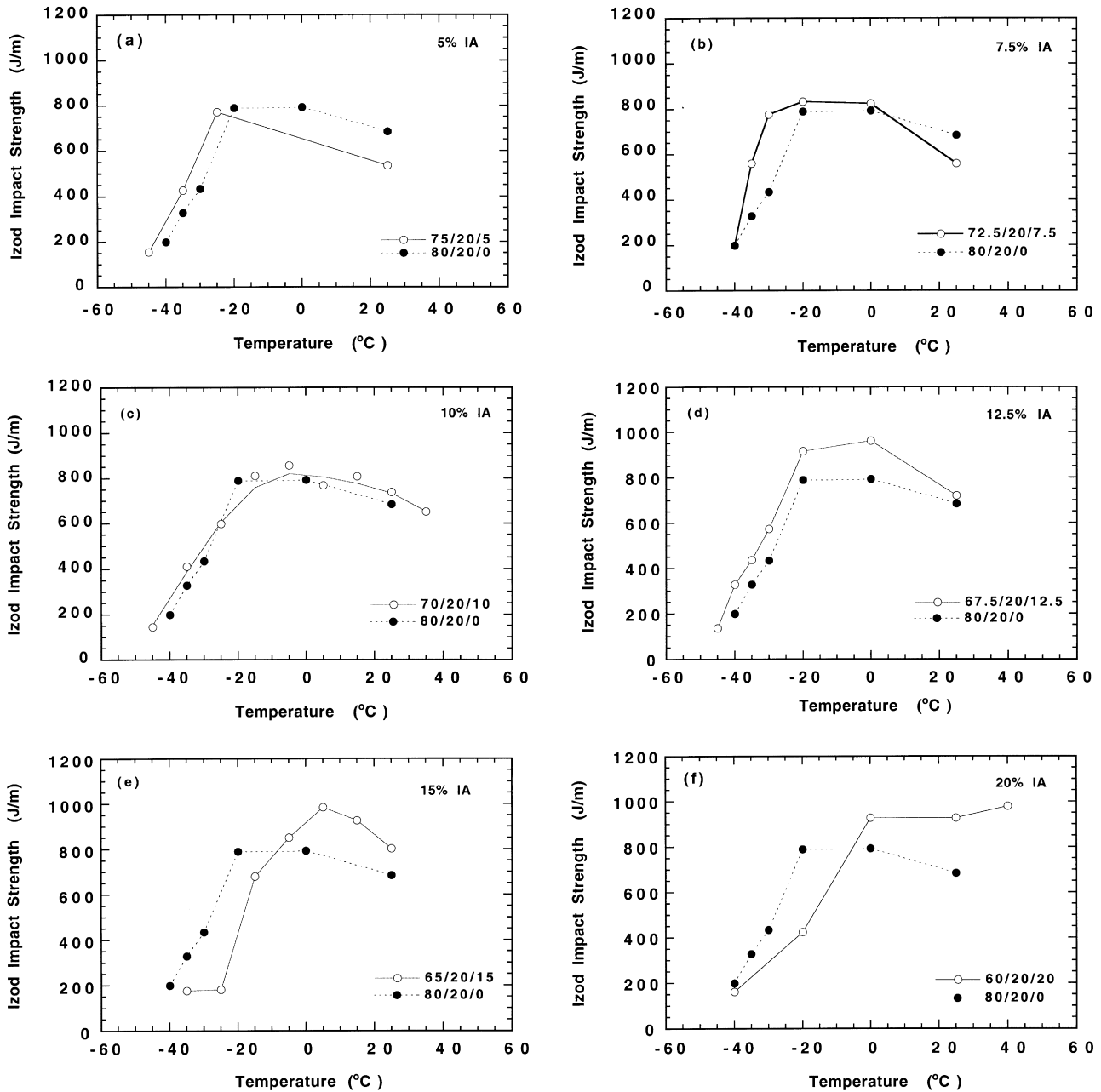


Fig. 8. Effect of temperature on the Izod impact strength of ternary blends of nylon 6/EPR-g-MA/IA containing 20 wt% of EPR-g-MA and the following amounts of IA: (a) 5%, (b) 7.5%, (c) 10%, (d) 12.5%, (e) 15%, (f) 20%. Each of the ternary blends is compared to an 80/20 nylon 6/EPR-g-MA blend.

data station at a heating rate of 20°C min<sup>-1</sup> using 5–15 mg samples trimmed from Izod bars.

### 2.1. Blends based on EPR-g-MA

This section describes the effects of varying the EPR-g-MA and imidized acrylic polymer concentrations in blends with nylon 6 on the rheology and mechanical properties of these materials. The imidized acrylic polymer and EPR-g-MA both react with nylon 6 [13,23] but are immiscible with each other and form separate dispersed phases.

#### 2.1.1. Rheology

Brabender torque rheometry was utilized to characterize the melt-flow behavior of these materials. The torque reported here is the value obtained for each blend after 10 min of mixing. Fig. 1 shows characteristic torque values of binary nylon 6/EPR-g-MA and nylon 6/IA blends as well as some ternary nylon 6/EPR-g-MA/IA blends. It is clear that nylon 6/IA blends have much higher melt viscosity than nylon 6/EPR-g-MA blends. Given that the molar concentrations of the anhydride units in the IA and EPR-g-MA materials are approximately equal, this suggests that the glutaric anhydride groups of IA are much more reactive with amine

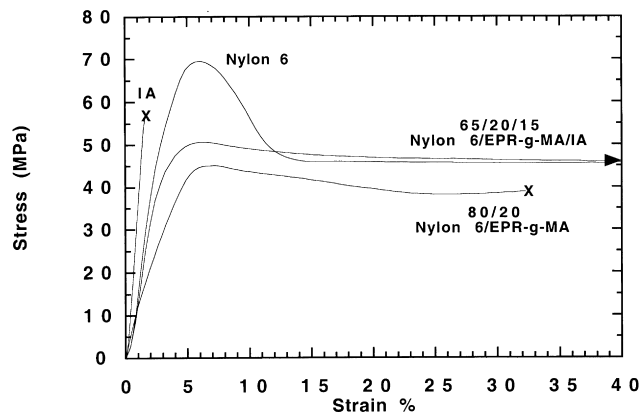


Fig. 9. Typical stress–strain curves for a binary nylon 6/EPR-g-MA blend and ternary nylon 6/EPR-g-MA/IA blend relative to pure nylon 6 and IA.

end groups of nylon 6 than the maleic anhydride groups of EPR-g-MA. Ternary blends have about the same torque as binary nylon 6/IA blends of the same nylon 6 content; apparently the effect of the imidized acrylic polymer on melt viscosity is enhanced even further in the ternary blends.

### 2.1.2. Nylon 6/EPR-g-MA binary blends

Fig. 2 shows that Young's modulus of binary blends of nylon 6 with EPR-g-MA decreases with increasing rubber content as expected. The room-temperature impact strength is dramatically improved relative to neat nylon 6 when the rubber content is 20% by weight or higher (see Fig. 3); the room-temperature impact strength is relatively constant in the range from 20% to 40% EPR-g-MA. As seen in Fig. 4, the blend which contains 20% rubber has a distinct ductile–brittle transition temperature at about  $-30^{\circ}\text{C}$ , while the blends with higher rubber content remain tough down to at least  $-55^{\circ}\text{C}$ . The improved low-temperature impact strength of the high rubber blends relates to the fact that the yield stress increases as the temperature is reduced but the deformation mode remains ductile. Super-tough nylon 6 blends typically contain of the order of 20% rubber giving

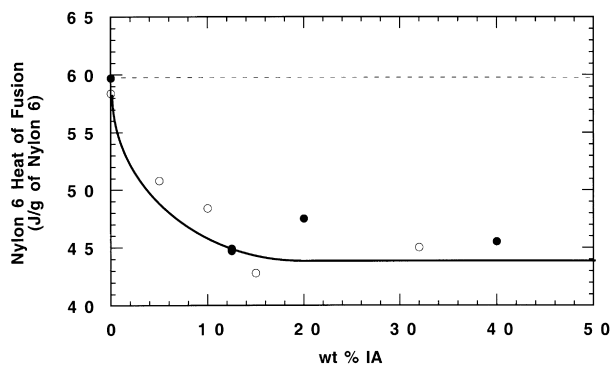


Fig. 10. Heat of fusion for nylon 6 in binary nylon 6/IA (●) and ternary nylon 6/EPR-g-MA/IA blends containing 20% EPR-g-MA (○) as a function of IA content. The heat of fusion was calculated from the area under the nylon 6 melting peak using DSC.

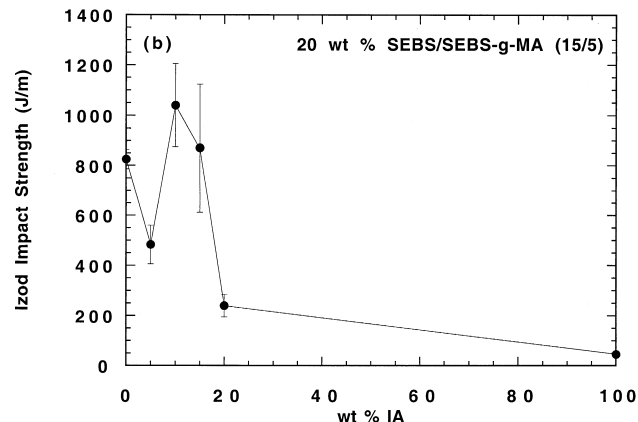
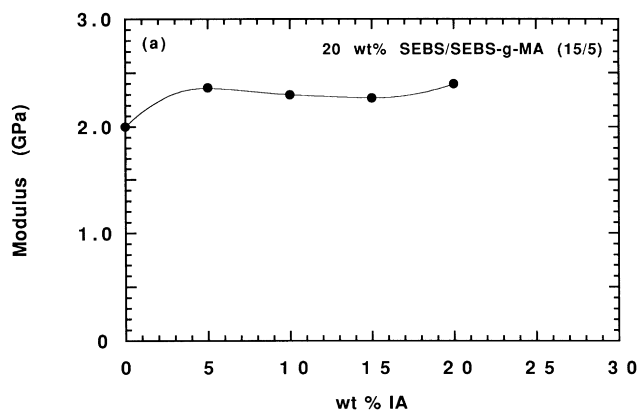


Fig. 11. Mechanical properties of nylon 6/(SEBS/SEBS-g-MA)/IA blends containing 20% of SEBS/SEBS-g-MA (15/5) as a function of IA content: (a) tensile modulus, (b) room-temperature Izod impact strength.

rise to materials with a reasonably good balance of low-temperature toughness and modulus. All ternary blends described here contain a fixed rubber content of 20 wt%.

### 2.1.3. Nylon/IA binary and nylon 6/EPR-g-MA/IA ternary blends

A series of blends of varying ratio of nylon 6 to imidized acrylic polymer and fixed EPR-g-MA (0 or 20%) content were prepared by adding all these ingredients simultaneously to the single-screw extruder. The moduli of these materials are shown in Fig. 5. As imidized acrylic polymer is added to nylon 6 in the absence of any EPR-g-MA, a rapid rise in modulus is obtained up to about 15–25% followed by a gradual decrease as more imidized acrylic is added up to about the 40% level. Above 40%, the modulus increases again up to 100% IA. The morphology of these binary blends is described in a later section.

This large stiffening effect observed for binary nylon 6/IA blends is also reflected in ternary nylon 6/EPR-g-MA/IA blends. The blends containing 20% rubber show the same tendency when IA is added; there is a rapid rise in modulus as the imidized acrylic is added up to about 15–20% (rubber-free basis) followed by a gradual decrease in modulus as more imidized acrylic is added up to about the 40% level. The room-temperature impact strength of the ternary

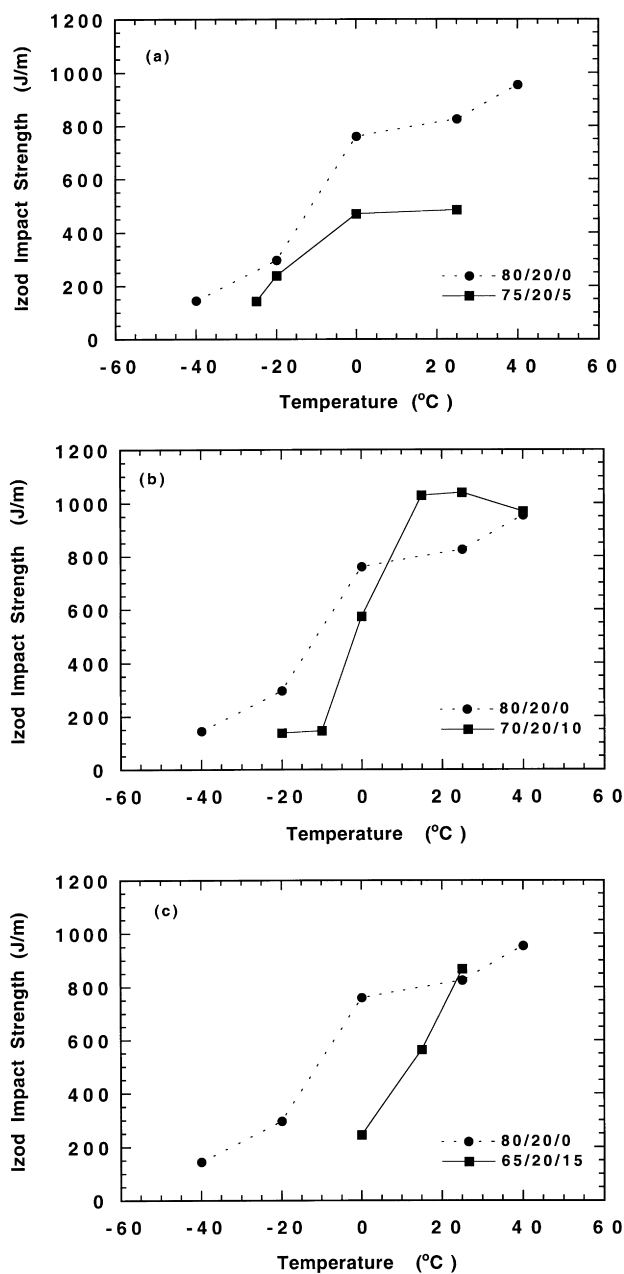


Fig. 12. Effect of temperature on impact strength of nylon 6/(SEBS/SEBS-g-MA)/IA blends containing 20% of SEBS/SEBS-g-MA (15/5) and the following contents of IA: (a) 5%, (b) 10%, (c) 15%. Each of the blends is compared to an 80/20 nylon 6/(SEBS/SEBS-g-MA) blend.

blends is shown in Fig. 6, for a fixed content of EPR-g-MA but a varying ratio of imidized acrylic polymer to nylon 6. Incorporation of a small amount of the imidized acrylic results in a decrease in impact strength. This decrease is followed by a rapid increase in impact strength as the content of the imidized acrylic is increased to about 25% on a rubber-free basis. As the imidized acrylic content is increased further, the ternary blends show an abrupt ductile-to-brittle transition. At this point, we cannot offer a rational explanation for the initial decrease in impact strength; however, it is evident that this reduction in toughness is

real (note error bars in Fig. 6). It will be demonstrated later that a similar trend exists for corresponding blends based on SEBS elastomers. Note that in Figs 5 and 6, the content of the imidized acrylic material in the ternary blend is given on a rubber-free basis to facilitate comparison with the binary blend containing no rubber; however, in subsequent plots, the IA content is expressed as a percentage,  $x$ , of the total ternary blend mass.

It is evident that the incorporation of the imidized acrylic polymer to super-tough nylon 6 affects the balance between stiffness and toughness in these blends. In Fig. 7, the values of Izod impact strength and modulus are replotted to emphasize this point; both properties are increased for some IA contents. A ternary blend containing 15% of the imidized acrylic polymer is about 32% stiffer (its modulus is only 10% lower than that of neat nylon 6) and about 22% higher in Izod impact strength at room temperature than the blend without this component. Furthermore, addition of IA does not change the good low-temperature impact properties of nylon 6/EPR-g-MA blends. In fact, as seen in Fig. 8, up to 12.5% content of IA, the ductile–brittle transition temperatures are lower than the binary nylon 6/EPR-g-MA blends. Increasing the IA content above 12.5%, however, reduces low-temperature toughness (note Fig. 8). No doubt the increase in Izod impact strength that accompanies the addition of the imidized acrylic polymer in these blends is due to the increase in stress during fracture as expected from stress–strain data like those shown in Fig. 9. It is interesting to note that the ternary blend containing 15% imidized acrylic polymer has a yield strength and elongation at break significantly higher than that of the binary 80% nylon 6/20% EPR-g-MA blend.

Grafting of nylon 6 chains to the rubber or to the imidized acrylic polymer is expected to reduce the crystallization rate of nylon 6 [34–37]; thus, the extent of nylon 6 crystallization may be reduced during the time of injection molding. Differential scanning calorimetry (DSC) was used to consider this possibility. Fig. 10 shows the heat of melting of the nylon 6 as a function of the amount of imidized acrylic polymer in the binary nylon 6/IA and ternary nylon 6/EPR-g-MA/IA blends obtained from first scans of specimens excised from an injection molded bar. The dashed line corresponds to the heat of fusion of neat nylon 6; the data points would be expected to fall on this line if the crystallinity were not disrupted by incorporation of the dispersed phase(s). It is evident that the crystallinity of nylon 6 is reduced due to grafting reactions. It is interesting to note that the binary nylon 6/EPR-g-MA blend does not have a significantly lower heat of fusion than nylon 6 itself, incorporation of the IA reduces the crystallinity to a much greater extent. This may be related to the higher degree of reaction of nylon 6 with the IA material relative to EPR-g-MA (note Fig. 1), or the lower mobility of the rigid phase compared to the rubber. Although not shown here, a qualitatively similar trend of crystallinity reduction was observed for corresponding blends containing SEBS-based

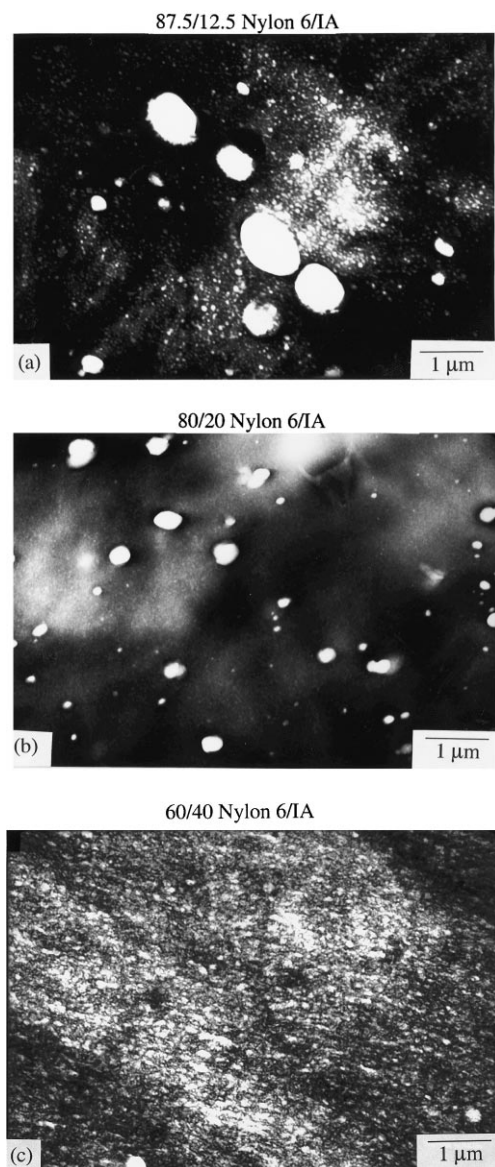


Fig. 13. TEM photomicrographs of blends of nylon 6 and IA containing the following amounts of IA: (a) 12.5%, (b) 20%, (c) 40%. The polyamide phase is stained dark by phosphotungstic acid (PTA).

elastomers. Other things being equal, a reduction in crystallinity would tend to reduce modulus and yield strength but increase ductility. However, both the binary and ternary blends described earlier show a maximum modulus around 15% of IA (see Fig. 5). Based on these results, the stiffening effect caused by addition of IA seems to have a greater influence on the modulus of these materials than the reduction in crystallinity of the nylon 6 matrix.

## 2.2. Blends based on SEBS-g-MA

This section describes the mechanical properties of blends toughened by SEBS-g-MA. The SEBS-g-MA material used here contains 1.84 wt% maleic anhydride, which leads to rubber particles that are too small to toughen nylon

6. However, certain combinations of SEBS-g-MA and its unmaleated precursor, SEBS, give rise to super-tough blends with rubber particles comparable in size to blends with EPR-g-MA [10–14]. Accordingly, a mixture of 25% SEBS-g-MA and 75% SEBS was used to obtain the rubber phase (total rubber content of 20%) in all blends based on SEBS-g-MA.

The response of the mechanical properties of nylon 6 toughened by the mixtures of SEBS-g-MA and SEBS to the addition of the imidized acrylic polymer is quite similar to the blends based on EPR-g-MA. The modulus and impact strength of these blends are shown in Fig. 11(a,b), respectively. As imidized acrylic polymer is added to the blend, the modulus increases slightly and then remains essentially constant up to 20 wt%. The room temperature Izod impact strength decreases significantly on addition of 5 wt% of IA; however, blends containing 10 and 15 wt% of IA have higher impact strength than those without IA. Blends containing more than 15 wt% IA are brittle. A qualitatively similar response is seen in Fig. 6 for blends toughened by EPR-g-MA. It is interesting to note that addition of 10% of IA leads to a material that is 15% stiffer (its modulus is only 10% lower than neat nylon 6) and 26% tougher than the nylon 6/(SEBS/SEBS-g-MA 15/5) 80/20 blend.

While the room-temperature impact properties of blends containing SEBS/SEBS-g-MA mixtures show the same qualitative trends as those based on EPR-g-MA, the low-temperature toughness of the former is not nearly as good as that of the latter. Fig. 12 compares the impact strength versus temperature curves for nylon 6/(SEBS/SEBS-g-MA 15/5)/IA versus those for nylon 6/(SEBS/SEBS-g-MA 15/5) 80/20 blends. It is clear that addition of IA to the SEBS-based blends is detrimental to the low-temperature impact properties. Cavitation of rubber particles seems to play a significant role in toughening matrices like nylon 6, and there is evidence that EPR-g-MA particles cavitate more readily than do SEBS-based particles [38]. This may play some role in the differences in impact properties of the two rubber types.

## 2.3. Morphology

In this section, the morphology of binary nylon 6/IA blends and ternary nylon 6/rubber/IA blends containing EPR-g-MA and SEBS/SEBS-g-MA rubbers are explored.

### 2.3.1. Binary nylon/IA blends

It was demonstrated earlier that the stiffness of binary nylon 6/IA blends was highly dependent on the blend composition (note Fig. 5); a maximum in the modulus was observed at 20 wt% IA. To determine the morphological nature of these materials, binary nylon 6/IA blends of the compositions of interest were examined. Fig. 13 shows TEM photomicrographs of binary blends containing 12.5, 20, and 40 wt% IA. The blend containing 12.5 wt% IA contains some large IA particles; these particles become

Ternary EPR-g-MA blends stained by solvent treatment method with  $\text{RuO}_4$  and PTA:

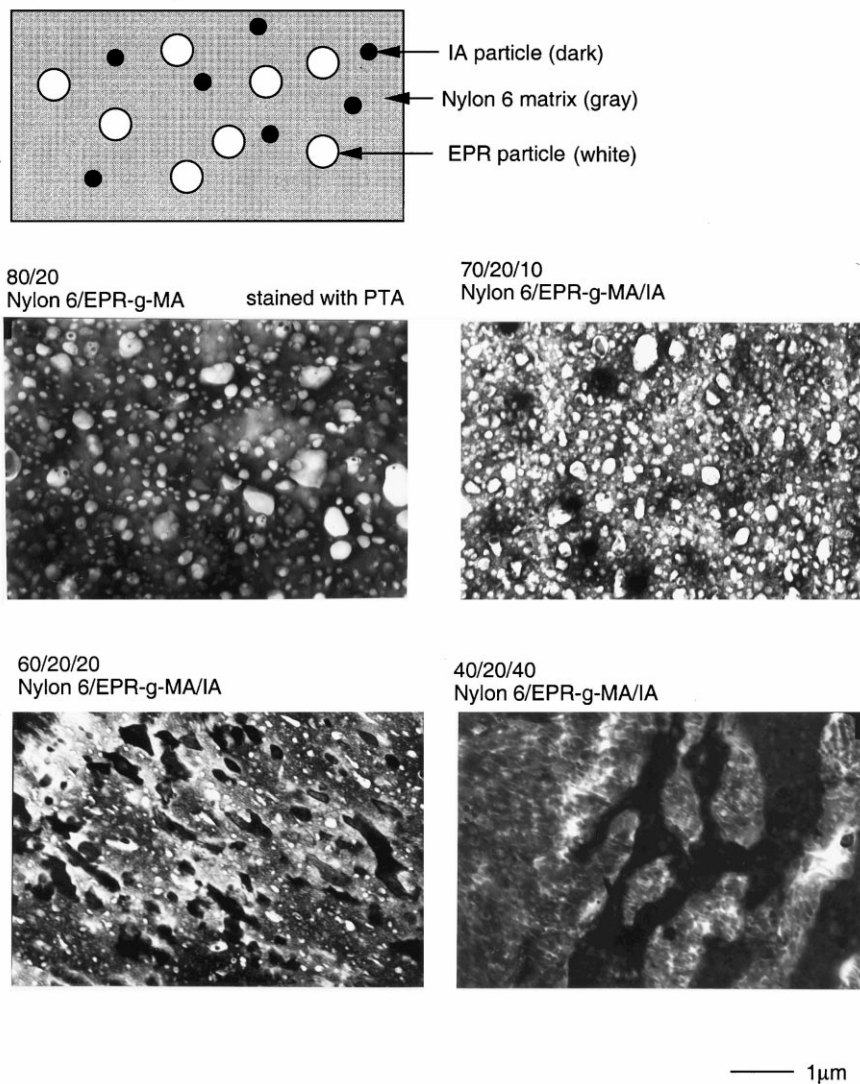


Fig. 14. TEM photomicrographs of blends based on nylon 6, IA, and EPR-g-MA.

smaller as the IA content is increased to 20 wt% (see Fig. 13(b)). As the IA content is increased further, the particles become even smaller (note Fig. 13(c)), and the blend has a co-continuous morphology. One would expect an increase in modulus if the rigid IA phase formed a co-continuous structure; however, the blend having the highest modulus (20 wt% IA) contains IA particles that are dispersed (see Fig. 13(b)). It is also unusual that the IA domains become smaller with increasing IA content. One would expect to observe larger IA domains with increasing IA content simply based on their volume fraction. It is possible that these domains become smaller as the amount of IA is increased due to the higher degree of grafting that can occur during melt processing (note Fig. 1); the increased rheological stress on the dispersed phase would tend to produce smaller IA domains. At this point, it is difficult to unambiguously resolve the relationship between

composition and microstructure among these binary blends; the maximum in modulus at 20 wt% IA is not fully explained by the blend morphology.

### 2.3.2. Ternary nylon 6/rubber/IA blends

The morphology of the ternary blends of nylon 6 containing various amounts of imidized acrylic polymer and toughened by a fixed amount of EPR-g-MA (Fig. 14) or SEBS-based rubber (Fig. 15) is illustrated by typical electron photomicrographs and schematic interpretations. Each ternary blend shows separate dispersed particles of the hard- and soft phases in the nylon 6 matrix. The rubber particles are white in Fig. 14 and black in Fig. 15, due to the different staining responses, as indicated by the appropriate schematics. The weight average diameter of each particle type was calculated by image analysis of the TEM photomicrographs, and the results are summarized in Fig. 16. The

Ternary SEBS-g-MA blends stained with PTA and RuO<sub>4</sub>:

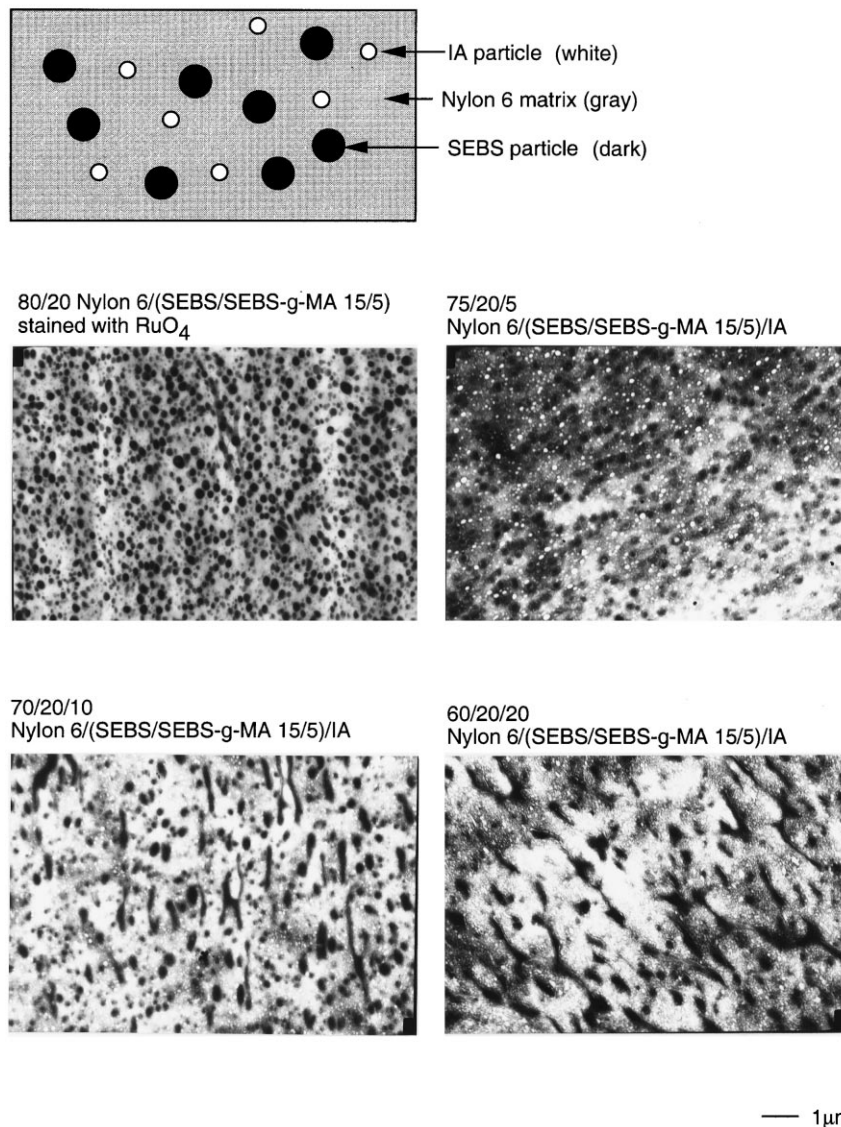


Fig. 15. TEM photomicrographs of blends based on nylon 6, IA, and a SEBS/SEBS-g-MA (15/5) mixture.

dispersed particles deviate somewhat from a perfectly round shape as may be seen in Figs 14 and 15. To characterize particle shape, the average ratio of the major axis to the minor axis of each particle type was computed; these aspect ratios are shown in Fig. 17. Trends in the changes in the size and shape of the soft and rigid particles offer some insights into the mechanical response observed for these blends.

For the blends based on EPR-g-MA, the rubber particles remain nearly constant in size at about 0.18 μm until the imidized acrylic polymer content exceeds 20% and then become larger. The hard particles continuously increase in size as the imidized acrylic polymer content is increased. Both the rubber particles and the IA particles become increasingly more elongated as the imidized acrylic polymer content increases. Below about 15% IA, the hard particles are smaller than the rubber particles. In the region of

optimum performance of these blends, the rubber particles remain small but are larger than the hard particles. The loss of toughness occurs in the region of IA content where the absolute rubber-particle size begins to increase and the hard particles become larger than the soft particles. It appears that the stiffening benefit caused by the hard phase is lost due to the IA tending to become the continuous phase. This is initially indicated by a more elongated shape at higher content of the imidized acrylic polymer.

For the blends based on SEBS-g-MA, the rubber particles are initially smaller than those based on EPR-g-MA but continuously increase in size (see Fig. 16(b)) and aspect ratio (see Fig. 17(b)) as imidized acrylic polymer is added. On the other hand, the hard-phase particles remain relatively constant in size and in aspect ratio as the IA content increases. Thus, for this system the rubber particles

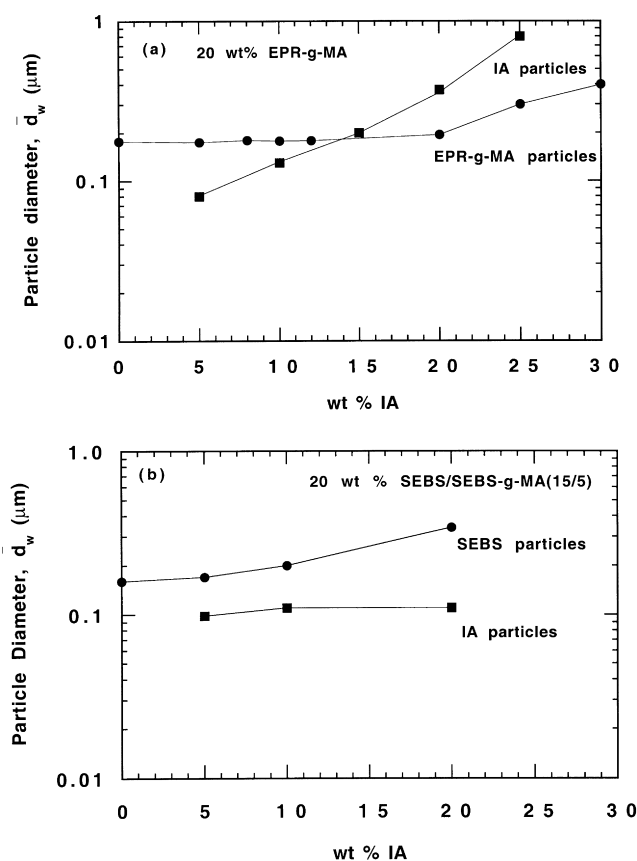


Fig. 16. Effect of IA content on the weight average particle diameter,  $\bar{d}_w$ , of the dispersed rubber phase (●) and IA phase (■) for blends containing (a) EPR-g-MA and (b) SEBS/SEBS-g-MA (15/5).

are always larger than the hard-phase particles. In general, the SEBS-based rubber seems to have a greater tendency to form the continuous phase (more elongated particles) than the EPR-g-MA rubber. For these materials, the properties become much worse when the rubber tends to be the continuous phase.

At this point, these morphological observations do not provide the basis for a full understanding of the large differences in the changes in stiffness and toughness of nylon 6 blends with EPR-g-MA versus those with SEBS-based rubber as imidized acrylic polymer is added. Another difference in the two rubber types is that SEBS-g-MA rubber is stiffer at room temperature than EPR-g-MA [14], and this is reflected in the higher modulus of binary blends of nylon 6 with the former (Fig. 11a) compared to the latter (see Fig. 4). This fact is mentioned merely to emphasize that no doubt an array of complex issues are involved in the behavior of these blend systems, of which morphology is only one.

#### 2.4. Effect of mixing protocol

The ternary blends described above were prepared by simultaneously adding all components to the extruder. A limited study of the sensitivity of the mechanical properties of these blends to the sequence of mixing the components

was conducted. Two different compositions were prepared containing 20% EPR-g-MA but different nylon 6/IA ratios; one composition contained 10% of the imidized acrylic polymer which is within the optimum performance range (see Figs 7 and 8) while the other contained 25% of the imidized acrylic polymer. The latter level of the imidized acrylic polymer exceeds the amount that showed ductile behavior (see Fig. 6) for blends prepared by the simultaneous addition method. Samples designated as A were made by mixing nylon 6 and EPR-g-MA in a first extrusion followed by adding the IA in a second extrusion. Samples designated as B were prepared by mixing nylon 6 and IA in a first extrusion and then adding the EPR-g-MA in a second extrusion. The mechanical properties are compared in Table 2 with those of blends of the same composition made by mixing all components simultaneously and extruding twice. The blends based on 10% IA showed the same excellent mechanical properties regardless of the method of preparation. However, for the blends containing 25% IA, the degree of toughness observed was rather sensitive to the method of preparation with method A giving much better properties.

The differences in Table 2 can be rationalized in terms of the total anhydride to amine end-group stoichiometry. As mentioned earlier, the anhydride units in both the rubber and hard phases react with nylon 6 amine end groups, and the resulting graft copolymers play a major role in determining the morphology formed. The anhydride units in these two phases must compete for the available amine groups in nylon 6, which becomes especially important when the total molar anhydride content of the blend exceeds the available amine end groups in nylon 6. This competition is influenced also by the intrinsic differences in reactivity of the glutaric anhydride units of the imidized acrylic polymer compared to the grafted maleic anhydride units in EPR-g-MA or SEBS-g-MA. Using the compositional information shown in Table 1, the molar ratio of total anhydride to amine groups was calculated as a function of imidized acrylic polymer content of ternary blends based on 20% EPR-g-MA or 15% SEBS and 5% SEBS-g-MA (see Fig. 18). Interestingly, for the EPR-g-MA based blends, this ratio is near unity at about 15% IA, where a good balance of properties is observed (see Figs 5–7). The deficiency of amine end groups at higher IA contents could be responsible for the morphological change observed in this region and, in turn, the deterioration in mechanical performance. In this region the anhydride units in the hard and soft phases must compete for reaction with the available amine chain ends, and it may not be possible to maintain size control of both particle types.

On the other hand, for all blends based on the 15% SEBS and 5% SEBS-g-MA mixture examined here, this molar ratio is less than unity, which means there are enough amine groups available for reaction with all anhydride units present; thus, stoichiometry may not play a very significant role in determining the properties of these blends. A full understanding of this system would require studies with

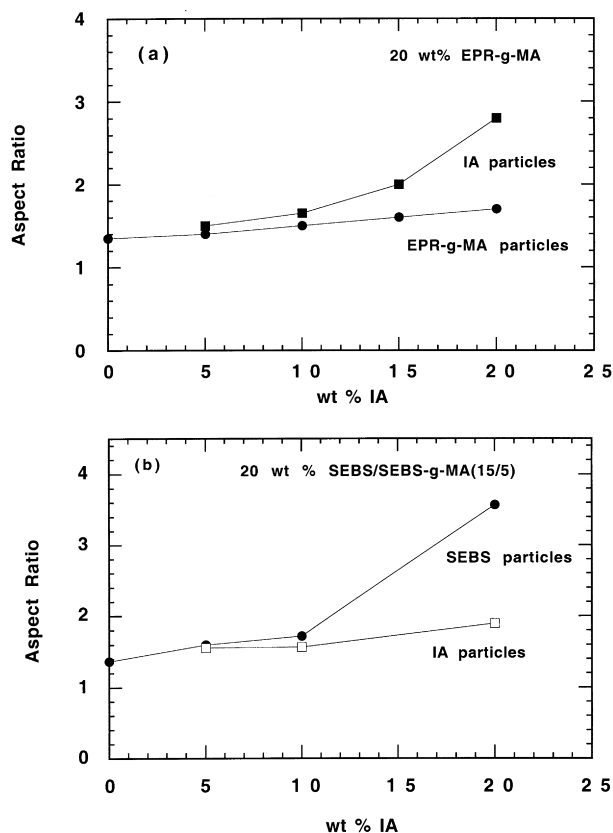


Fig. 17. Effect of IA content on the aspect ratio of the dispersed rubber phase (●) and IA phase (■) particles for blends containing (a) EPR-g-MA and (b) SEBS/SEBS-g-MA (15/5).

a series of rubbery and hard-phase materials whose functionality is varied over appropriate ranges. It would be especially important to include SEBS-g-MA materials which have lower levels of maleation that lead to super-tough blends with nylon 6 without resorting to dilution with unmaled SEBS [10].

The order of mixing the components can also affect the

Table 2  
Effect of mixing order on blend properties

Blend	Mixing order	Izod impact strength (J/m)	Modulus (GPa)	Yield Strength (MPa)	Ductile–brittle transition temperature (°C)
Nylon 6/ EPR-g-MA/ IA 70/20/10	Simultaneously mixed	738	2.16	47.3	–35
	Method A <sup>a</sup>	617	2.13	47.7	–35
	Method B <sup>b</sup>	681	1.87	47.0	–35
Nylon 6/ EPR-g-MA/ IA 55/20/25	Simultaneously mixed	374	1.88	44.2	25
	Method A <sup>a</sup>	928	2.31	49.4	–10
	Method B <sup>b</sup>	57	1.35	35.2	45

<sup>a</sup> Method A: 1st extrusion Nylon 6/EPR-g-MA; added IA in 2nd extrusion.

<sup>b</sup> Method B: 1st extrusion Nylon 6/IA; added EPR-g-MA in 2nd extrusion.

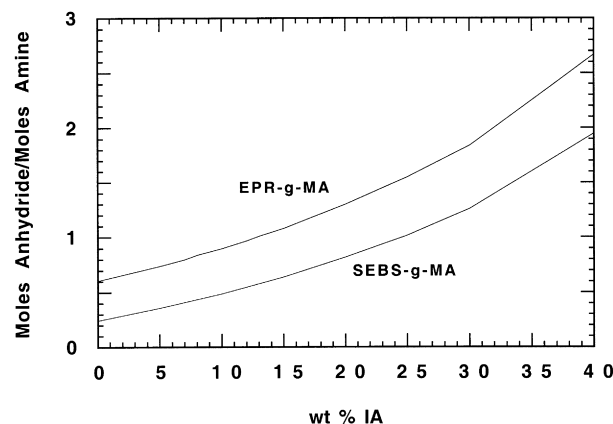


Fig. 18. Ratio of total moles of anhydride groups (from IA and rubber) to amine end groups of nylon 6 as a function of IA content for ternary blends of nylon 6/rubber/IA containing 20 wt% rubber. The molar ratio of anhydride to amine groups is calculated using data in Table 1.

extent of amine group reactions between the hard versus soft phases. Fig. 19 shows the molar ratio of anhydride to amine groups as a function of the dispersed phases (EPR-g-MA or IA) considering only the binary blends with nylon 6. The points on these curves correspond to the ratio of nylon 6 to the dispersed phase in a first-pass extrusion; i.e. 70/10 nylon 6/IA corresponds to 12.5 wt% IA in the first extrusion. The ratio of anhydride to amine at these points governs the amount of amine end groups that can be consumed prior to the second extrusion, with a value of unity corresponding to a complete depletion of amine end groups if the reaction proceeds to completion. It is interesting to note that when there are more amine end groups than anhydrides available for reaction after a first-step extrusion, i.e. nylon 6/EPR-g-MA 70/20 (method A) and nylon 6/IA 70/10 (method B), the blend properties are relatively insensitive to the mixing protocol. However, when the number of amine end groups and anhydrides are more nearly equal (note that the 55/20 nylon 6/EPR-g-MA and 55/25 nylon 6/IA points have a

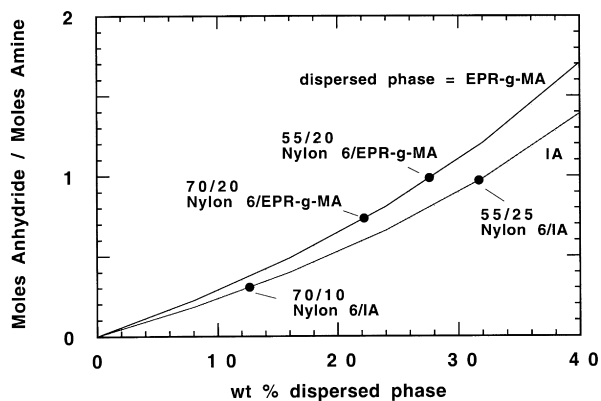


Fig. 19. Ratio of total moles of anhydride groups to amine end groups of nylon 6 for binary blends of nylon 6/EPR-g-MA and nylon 6/IA as a function of weight percent of the dispersed phase. The data points represent the ratio of nylon 6 to the dispersed phase in a first-pass extrusion, as indicated by the mixing protocols shown in Table 2.

molar ratio close to unity), the blend properties are very sensitive to the order of mixing. The best properties are obtained when the amine end groups are not limiting and a maximum amount of rubber is allowed to react with nylon 6 (method A); whereas, poorer properties result when the rubber has a limited opportunity to react (method B). In this particular case, it is clear that varying the order of mixing offers a powerful means to obtain desirable mechanical properties.

### 3. Conclusions

Ternary blends containing separate phases of soft (EPR-g-MA or SEBS/SEBS-g-MA) and hard (imidized acrylic polymer) particles were examined. Super-tough blends based on EPR-g-MA showed increased stiffness and impact strength as IA was added within a certain composition range. The good low-temperature impact properties of binary nylon 6/EPR-g-MA blends were retained as the imidized acrylic polymer was added up to a critical level; beyond this critical IA content, these properties were dramatically reduced. When mixtures of SEBS and SEBS-g-MA were used as the rubber instead of EPR-g-MA, similar improvements in room-temperature mechanical properties were observed. However, the low-temperature impact properties were compromised. These simultaneous improvements in stiffness and toughness are examined in terms of blend morphology and chemical stoichiometry; however, a full understanding of these important property enhancements is not available at the present time.

### Acknowledgements

This research work was supported by the US Army

Research Office and Mitsubishi Gas Chemical Co. Inc. The authors express their appreciation to AlliedSignal Inc., Exxon Chemical Co., Rohm and Haas Co. and Shell Development Co. for providing the various materials used in this research.

### References

- [1] Lawsen DF, Hergenrother WL, Matlock MG. *J Appl Polym Sci* 1990;39:2331.
- [2] Gilmore DW, Modic MJ. *Plastics Eng* 1989;45(4):51.
- [3] Wu SJ. *Appl Polym Sci* 1988;35:549.
- [4] Borggreve RJM, Gaymans RJ, Schuijjer J, Ingen Housz JF. *Polymer* 1987;28:1489.
- [5] Borggreve RJM, Gaymans RJ. *Polymer* 1989;30:63.
- [6] Borggreve RJM, Gaymans RJ, Schuijjer J. *Polymer* 1989;30:71.
- [7] Borggreve RJM, Gaymans RJ, Eichenwald HM. *Polymer* 1989;30:78.
- [8] Epstein BN. US Patent No. 4174358 (to EI DuPont), 1979.
- [9] Wu S. *Polym Eng Sci* 1987;27:335.
- [10] Oshinski AJ, Keskkula H, Paul DR. *Polymer* 1992;33:268.
- [11] Oshinski AJ, Keskkula H, Paul DR. *Polymer* 1992;33:284.
- [12] Oshinski AJ, Keskkula H, Paul DR. *Polymer* 1996;37:4891.
- [13] Oshinski AJ, Keskkula H, Paul DR. *Polymer* 1996;37:4909.
- [14] Oshinski AJ, Keskkula H, Paul DR. *Polymer* 1996;37:4919.
- [15] Datta S, Lohse DJ, editors. *Polymeric compatibilizers (section B5)*. New York: Hanser, 1996.
- [16] Keskkula H, Paul DR. *Toughened nylons*. In: Kohan MI, editor. *Nylon plastics handbook (Chapter 11, Section 6)*. New York: Hanser/Gardner, 1995.
- [17] Fujita Y, Koo KK, Angola JC, Inoue T, Sakai T. *Kobunshi Ronbunshu* 1986;43:119.
- [18] Koo KK, Inoue T, Miyasaka K. *Polym Eng Sci* 1985;25:741.
- [19] Angola JC, Fujita Y, Sakai T, Inoue T. *J Polym Sci, Part B: Polym Phys* 1988;26:807.
- [20] Kurauchi T, Ohta T. *J Mater Sci* 1984;19:1699.
- [21] Keitz JD, Barlow JW, Paul DR. *J Appl Polym Sci* 1984;29:3131.
- [22] Keskkula H, Paul DR. In: Collyer AA, editor. *Rubber toughened engineering plastics (Chapter 5)*. London: Chapman and Hall, 1994.
- [23] Majumdar B, Keskkula H, Paul DR, Harvey NG. *Polymer* 1994;35:4263.
- [24] Majumdar B, Keskkula H, Paul DR. *Polymer* 1994;35:5453.
- [25] Majumdar B, Keskkula H, Paul DR. *Polymer* 1994;35:5468.
- [26] Majumdar B, Keskkula H, Paul DR. *J Polym Sci, Part B: Polym Phys* 1994;32:2127.
- [27] Lavengood RE, Silver FM. *Soc Plast Eng ANTEC* 1987;45:1369.
- [28] Kudva RA, Keskkula H, Paul DR. *Polymer* 1998;39:2447.
- [29] Lu M, Keskkula H, Paul DR. *Polymer* 1993;34:1874.
- [30] Lu M, Keskkula H, Paul DR. *Polym Eng Sci* 1994;34:33.
- [31] Lu M, Keskkula H, Paul DR. *J Appl Polym Sci* 1996;59:1467.
- [32] Koning C, Vondervoort LVD. *Soc Plast Eng ANTEC* 1992;38:1435.
- [33] Gonzalez-Montiel A. Ph.D. dissertation, University of Texas at Austin, 1994.
- [34] Gonzalez-Montiel A, Keskkula H, Paul DR. *Polymer* 1995;36:4587.
- [35] Ikkala OT, Holsti-Miettinen RM, Seppala J. *J Appl Polym Sci* 1993;49:1165.
- [36] Moon HS, Ryoo BK, Park JK. *J Polym Sci: Part B: Polym Phys* 1994;32:1427.
- [37] Martuscelli E, Riva F, Sellitti C, Silvestre C. *Polymer* 1985;26:270.
- [38] Gonzalez-Montiel A, Keskkula H, Paul DR. *Polymer* 1995;36:4621.